Linking large piezoelectric coefficients to highly flexible polarization of lead free BaTiO3-CaTiO3-BaZrO3 ceramics

Feres Benabdallah, Annie Simon, Hamadi Khemakhem, Catherine Elissalde, Mario Maglione

Linking large piezoelectric coefficients to highly flexible polarization of lead free $BaTiO_3$-$CaTiO_3$-$BaZrO_3$ ceramics

F. Benabdallah,[1,2] A. Simon,[2] H. Khemakhem,[1] C. Elissalde,[2] and M. Maglione[2,a)]
[1]*Laboratoire des Matériaux Ferroélectriques, Faculté des Sciences de Sfax, BP802, 3018 Sfax, Tunisia*
[2]*Institut de Chimie de la Matière Condensée de Bordeaux, CNRS-Université Bordeaux 1, 87, Avenue Dr. A. Schweitzer, 33608 Pessac, France*

(Received 16 March 2011; accepted 16 May 2011; published online 29 June 2011)

We report a large d_{31} piezoelectric coefficient and corresponding electromechanical coupling factor, K_p, of $0.5Ba(Zr_{0.2}Ti_{0.8})O_3$–$0.5(Ba_{0.7}Ca_{0.3})TiO_3$ (BCTZ50) and $0.68Ba(Zr_{0.2}Ti_{0.8})O_3$–$0.32(Ba_{0.7}Ca_{0.3})TiO_3$ (BCTZ32) lead-free piezoceramics. The piezoelectric coefficient, d_{31}, reaches a high value of 200 pC/N for BCTZ50 at room temperature which is comparable to the one of the soft PZT. This confirms the previously reported d_{33} for the same material. A useful way to achieve such performances at the expense of a smaller thermal budget is suggested, enabling better control of the ceramics composition and microstructure. Based on pyroelectric and ferroelectric hysteresis loops measurements, we show that such outstanding properties are likely due to the high flexibility of polarization under thermal and electric stresses. © *2011 American Institute of Physics*. [doi:10.1063/1.3599854]

I. INTRODUCTION

Piezoelectric materials may be used either to generate charges under stress (the direct effect) or to induce strain under an electric field (the reverse effect). Two types of contributions to the net piezoelectric response are usually distinguished: one type is called an intrinsic contribution, and it is due to the distortion of the crystal lattice under an applied electric field or a mechanical stress.[1] The second type is called an extrinsic contribution, and it results from the motion of domain walls or domain switching.[2,3] At present the most important piezoelectric materials that are technologically interesting are ferroelectric ceramics based on Pb-containing perovskites such as lead-zirconate-titanate (PZT), close to 50/50 mixing of tetragonal $PbTiO_3$, and rhombohedral $PbZrO_3$. The strong piezoelectric ability of PZT relies on this balanced mixing between two different symmetries leading to a high polarization flexibility (polarization rotation between equivalent ferroelectric states under finite field). Depending on the model used, such flexibility may either come from the coexistence of several polarization orientations at the nanoscale[4] or from long range intermediate states/monoclinic/linking the parent tetragonal and rhombohedral states.[5,6] Based on both of these models, the quest for lead-free piezoelectrics relies on the mixing of several compatible structures in the same material leading to the construction of phase diagrams containing a morphotropic phase boundary, MPB (a region rising from a composition-induced phase transition between two ferroelectric phases) in which an extrinsic piezoelectric effect is expected to be giant.[7] This led to some success based on some high temperature ferroelectric materials free from lead [$(K,Na)NbO_3 + LiNbO_3$ (Refs. 8 and 9) and $(K,Na)NbO_3 + LiTaO_3 + LiSbO_3$ (Ref. 10)…]. Recently, Ren *et al*. have reported a high piezoelectric coefficient, d_{33}, of 620 pC/N in the lead-free solid solution $0.5(BaZr_{0.2}Ti_{0.8}O_3)$–$0.5(Ba_{0.7}Ca_{0.3}TiO_3)$, which is higher than the one for the ultra-soft PZT at room temperature.[11] This is a breakthrough since no lead-free ceramics could compete with this record up to now. In related studies, Li *et al*. have found significantly large dielectric and piezoelectric properties in $Ba_{1-x}Ca_x\ Ti_{0.95}Zr_{0.05}O_3$ with d_{33} and K_p rising up to 365 pC/N and 48.5%, respectively, for $x = 0.08$.[12]

Most importantly, all of the previously mentioned works highlight the original properties of the BCTZ lead-free ceramics. However, the low Curie temperature of these materials restricted their use for applications. For this reason, Bao *et al*. have designed a modified (1-x)BZT-xBCT system with higher T_c without altering their colossal electromechanical response.[13]

In this report, we focused our attention on the given compositions $0.68Ba(Zr_{0.2}Ti_{0.8})O_3$–$0.32(Ba_{0.7}Ca_{0.3})TiO_3$ and $0.5Ba(Zr_{0.2}Ti_{0.8})O_3$–$0.5(Ba_{0.7}Ca_{0.3})TiO_3$ which will be called BCTZ32 and BCTZ50, respectively, in the following text. The former composition corresponds to the triple point where a cubic non-ferroelectric phase can coexist with two ferroelectric phases of rhombohedral and tetragonal symmetry. The latter composition leads to a superposition of tetragonal and rhombohedral states close to room temperature.[11] While previous reports focused on the extremely large longitudinal d_{33} coefficients, here we show for the same compositions that the transverse d_{31} coefficients are also large enough to compete with PZT. The modeling of such appealing piezoelectric performances has been based mostly on the coexistence of several crystalline states. As a result, the degeneracy of many equilibrium states lead to a highly flexible polarization. In this report, we show that the polarization is continuously changing versus temperature in the ferroelectric state, thus confirming the flexibility of BCTZ ceramics.

a)Author to whom correspondence should be addressed. Electronic mail: maglione@icmcb-bordeaux.cnrs.fr.

II. EXPERIMENTAL PROCEDURES

The investigated compositions BCTZ32 and BCTZ50 were prepared by a conventional solid state reaction technique. Raw materials with stoichiometric fractions of $BaCO_3$ (99.95%), TiO_2 (99.9%), $CaCO_3$ (99.5%), and ZrO_2 (99.99%) were mixed and ground by ball milling for 2 h with the addition of alcohol. After drying, the mixture powders were calcined at 1350 °C for 15 h in an oxygen atmosphere.

The synthesized BCTZ powders were milled again, pressed under a uniaxial pressure of 120 MPa into sample disks, 8 mm in diameter and 1 mm in thickness, and sintered at 1400–1450 °C for 4 h under an oxygen atmosphere. An addition of 1% mol TiO_2 excess was used as a sintering aid for the two selected compositions.[14]

Room temperature powder x-ray diffraction was performed on a PANalytical X'Pert MPD diffractometer using the conventional θ-θ scan method. The x-ray tube delivers an incident beam containing Cu $K\alpha_1$ radiation of wavelength 1.54056 Å. The diffracted intensities were detected in the angle range $20 \leq 2\theta \leq 100$ with 600.075 s counting time for each step of 0.008° in order to measure Bragg angles and to determine the structure of our samples.

Dielectric measurements were performed on ceramic disks after the deposition of gold electrodes on the circular faces by cathodic sputtering. The dielectric permittivity of the sample was measured under helium atmosphere as a function of both temperature (80–500 K) and frequency (10^3–5.10^4 Hz) using an LCR meter (Wayne Kerr 4300). For piezoelectric measurements, the samples were set in a homemade cell and poled under a dc electric field of 8 kV cm^{-1} during cooling from the Curie temperature. The piezoelectric coefficients, along with the electromechanical coupling factors, were determined by the resonance method, mentioned in the IEEE standard on piezoelectricity using an HP4194 A impedance analyzer.[15] A Sawyer-Tower circuit with compensation of capacitance and resistance was used to follow the evolution of the ferroelectric hysteresis loops with temperature. Pyroelectric measurements were carried out with a digital multimeter (Keithley 2100) to determine the thermal variation of the spontaneous polarization. The pyroelectric current and the temperature of the poled sample (dc electric field ~10 kV cm^{-1}) were recorded simultaneously during heating between 150 and 450 K.

III. RESULTS AND DISCUSSION

A. X-ray diffraction analysis

Figure 1 shows the x-ray diffraction pattern of the BCTZ ceramics (with and without TiO_2 excess) at room temperature. No secondary phase is observed and all samples are perovskite-structured solid solutions. For both BCTZ32 and BCTZ50, the TiO_2 excess causes peaks to shift to higher angles which correspond to a contraction of the unit cell (Fig. 2). These results suggest that Ti^{4+} (the ionic radius $r(Ti^{4+}) = 0.605$ Å in octahedral coordination) arising from an excess of TiO_2 partially replace a small amount of Zr^{4+} ions ($r(Zr^{4+}) = 0.72$ Å in octahedral coordination) in the B-sites of the perovskite structure and lead to a decrease of the unit cell volume.[16,17] In this case, either Zr^{4+} or residual Ti^{4+} ions have to present at the grain boundaries and form a tiny amount of secondary phase. However, such an additional Zr/Ti-rich phase is not detectable either by x-ray diffraction or by electron probe microanalysis.

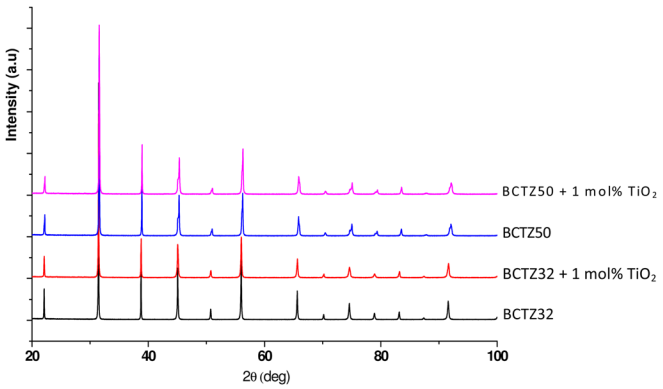

FIG. 1. (Color online) XRD pattern of BCTZ50 and BCTZ32 compositions with/without TiO_2 excess. No secondary phases occurred in both cases.

From the crystallographic point of view, the BCTZ50 could be indexed in the tetragonal symmetry (P 4 m m space group) either with or without TiO_2 excess. The lattice parameters and the unit cell volume are calculated using a global profile-matching method with the FullProf software and are listed in the following:

$$\text{BCTZ50} : a = b = 4.0005(5)\ \text{Å}, \quad c = 4.0173(3)\ \text{Å},$$
$$\alpha = \beta = \gamma = 90°, \quad V_{\text{Cell}} = 64.2949\ \text{Å}^3, \tag{1}$$

$$\text{BCTZ50} + 1\%\text{mol.TiO}_2\text{: } a = b = 3.9986(1)\ \text{Å},$$
$$c = 4.0187(5)\ \text{Å}, \quad \alpha = \beta = \gamma = 90°,$$
$$V_{\text{Cell}} = 64\ .2553\ \text{Å}^3. \tag{2}$$

It should be noted that the (200) peak broadening for the BCTZ50 point to a wide distribution of lattice parameters which could be attributed to locally different internal stresses in the material (Fig. 2), resulting from the coexistence of different structures at RT. This is consistent with the literature, in which the strong peak overlapping in BCTZ50 was correlated with the coexistence of the rhombohedral and tetragonal phase close to RT.[11]

For the triple point (BCTZ32), the structural characterization by standard XRD technique is much more complex. In fact, two ferroelectric phases with tetragonal and rhombohedral symmetry could coexist with a cubic non-ferroelectric one near RT (338 K). Our standard x-ray diffraction studies are, thus, in agreement with the previously reported coexistence of symmetries close to the triple point. Further experiments using high-resolution synchrotron x-ray powder diffraction are in progress to investigate the phase structure at the nanometric scale for both BCTZ32 and BCTZ50.

B. Dielectric study

As shown in Fig. 3, the dielectric permittivity displays a broad maxima at the expected transition temperature and is in good agreement with the diagram given in Ref. 11. We also

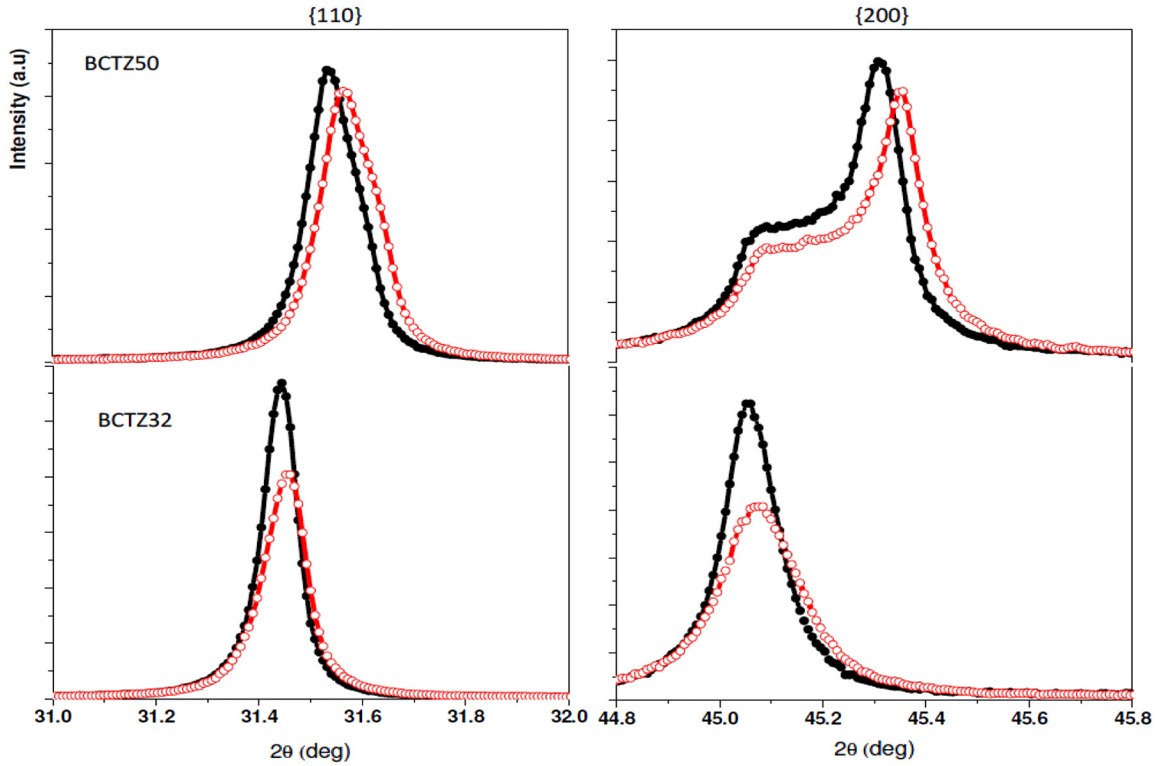

FIG. 2. (Color online) The (110) and (200) reflections for BCTZ 50 and BCTZ32 compositions. The filled and open circles represent peaks obtained without and with TiO2 excess, respectively. The peak shifting to higher angles corresponds to a contraction of the unit cell. The (200) peak broadening for BCTZ 50 may be attributed to a wide distribution of lattice parameters due to the coexistence of different structures.

observe that the maximum value of the dielectric permittivity is systematically much higher for samples with TiO_2 excess. This means that the addition of TiO_2 is a helpful processing parameter to obtain dense BCTZ ceramics and, consequently, to enhance the dielectric properties. The obtained densities were 90% of the theoretical values for standard samples (without TiO_2 excess) and such values were improved up to 96% (for BCTZ50 + 1 mol. % TiO_2) and 93% (for BCTZ32 + 1

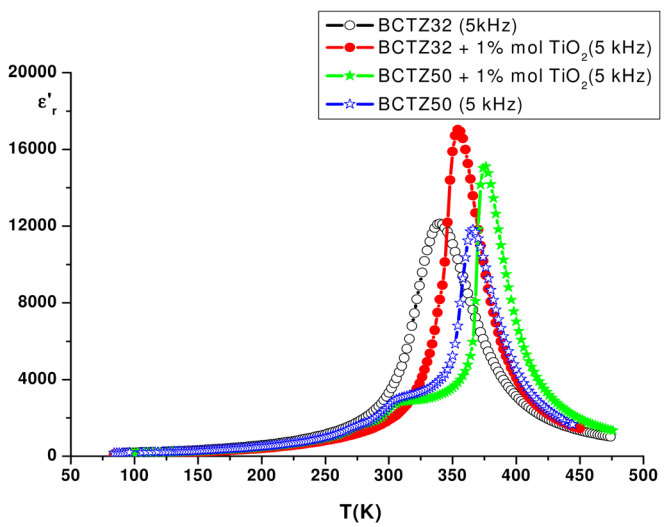

FIG. 3. (Color online) Temperature dependence of the real part ϵ'_r of the dielectric permittivity obtained for BCTZ ceramics at 5 kHz. Samples sintered with TiO_2 excess (● BCTZ32 and ⋆ BCTZ50) show a higher transition temperature and larger permittivity than those sintered without TiO_2 excess (○ BCTZ32 and ☆ BCTZ50).

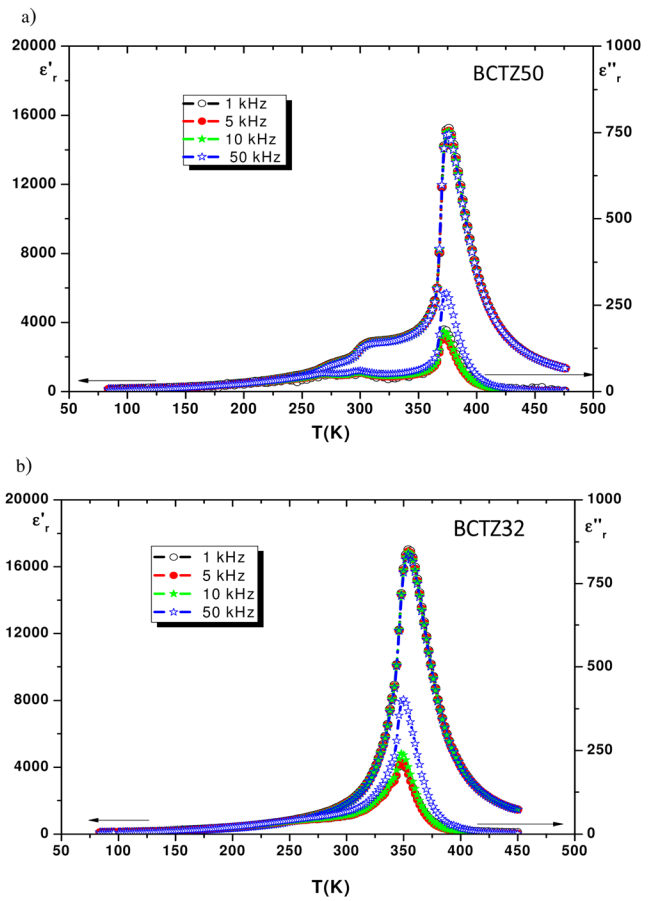

FIG. 4. (Color online) Temperature dependence of the real part ϵ'_r and the imaginary part ϵ''_r of the dielectric permittivity for (a) BCTZ50 and (b) BCTZ32 measured at different frequencies from 1 to 50 kHz.

mol. % TiO_2). The shift of the Curie temperature for compositions with TiO_2 excess probably results from the diffusion of Ti inside the host matrix of our samples during the sintering process. This is well-supported by the XRD measurements. As discussed in the preceding text, the decrease of the unit cell parameters with TiO_2 excess (Fig. 2) can be linked to a change of the Zr/Ti ratio in the B-site of the perovskite structure. In this case, the composition becomes slightly depleted of Zr and moves toward the rich $Ba_{0.7}$ $Ca_{0.3}$ TiO_3 region (as shown in the phase diagram)[11] and consequently causes T_c to shift to higher temperatures. In the following text, we will limit the discussion to samples with TiO_2 excess.

The temperature dependence of the real part ϵ'_r and imaginary part ϵ''_r of the dielectric permittivity in the frequency range of 1 to 50 kHz are presented in Figs. 4(a) and 4(b). For BCTZ50, the observed dielectric anomalies correspond to the phase transitions from a cubic paraelectric to a tetragonal ferroelectric (at $T_c = 376$ K) and to a rhombohedral ferroelectric (at $T_1 = 303$ K). However, only one dielectric peak was detected for BCTZ32 at ($T_c = 354$ K). This is consistent with the fact that this latter composition is close to the tricritical point of the phase diagram. For both compositions, the temperature where the dielectric peaks occur is not dependent on frequency, showing that these compounds are not relaxors. This is confirmed by the behavior of dielectric losses which stay low for all temperatures ($\tan \delta < 0.05$).

C. Piezoelectric characterization

The conductance, G, and the susceptance, B, in the radial vibration mode are presented through a room temperature impedance measurement for TiO_2 excess ceramics [Figs. 5(a) and 5(c)]. The fitting was achieved by using the standard equivalent circuit of Mason's model.[18] Using a linear frequency sweep at every temperature, the transverse piezoelectric coefficient, d_{31}, and the planar coupling factor, K_p, were computed and plotted versus temperature [Figs. 5(b) and 5(d)]. As shown, the excess TiO_2 is highly beneficial, leading to an enhancement of the piezoelectric coefficient, d_{31}, which reach levels as high as 120 pC/N for BCTZ32 and

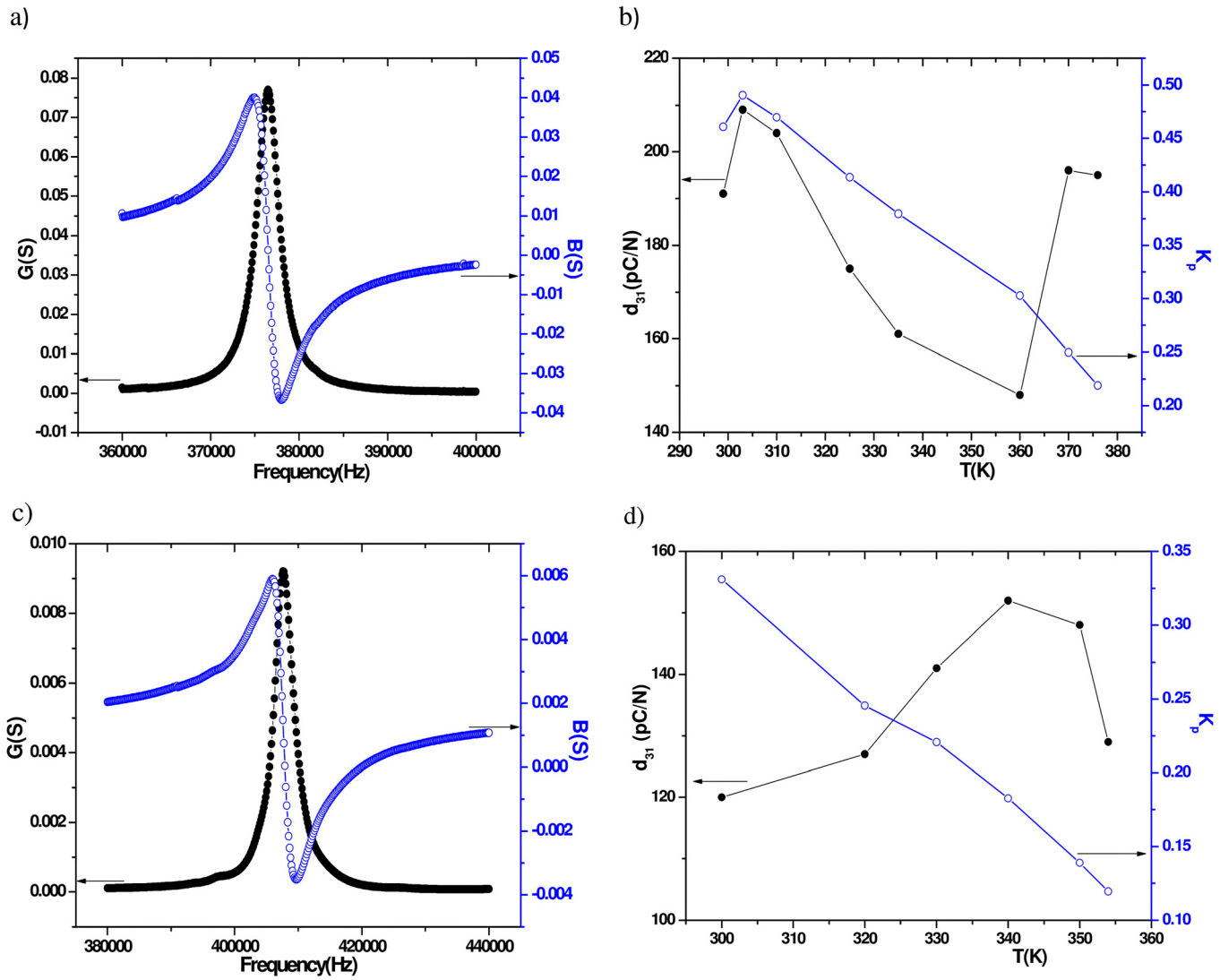

FIG. 5. (Color online) The conductance, G, and the susceptance, B, measured at room temperature for the radial vibration mode are plotted for (a) BCTZ50 and (c) BCTZ32. From such sweeps, the transverse piezoelectric coefficient, d_{31}, and the electromechanical coupling factor, K_p, were computed at every temperature. Thermal evolution of d_{31} and K_p for (b) BCTZ50 and (d) BCTZ32.

~200 pC/N for BCTZ50 at RT. These values compare well with those of hard and soft PZT, respectively.[19–21] Such colossal transverse coefficients and their maximum for BCTZ50 agree well with the previously published d_{33} parameters.[11] This also confirms that the lower sintering temperature which we used due to theTiO_2 excess as a sintering agent, is not altering the piezoelectric performances. Such large piezoelectric responses are believed to be associated with a flat free energy surface (that is. soft force constant for ferroelectric displacements) driving polarization rotation near the MPB line.[22]

While the coupling factor, K_p, is continuously decreasing upon heating, the piezoelectric coefficient, d_{31}, displays a broad maxima at the ferroelectric transition temperatures, which is in agreement with the dielectric behavior. Two maxima are observed for BCTZ50 at the rhombohedral-tetragonal ($d_{31} \sim 210$ pC/N) and cubic-tetragonal ($d_{31} = 195$ pC/N) transition temperatures, and a single and broad maximum is observed for BCTZ32 ($d_{31} \sim 152$ pC/N). A high electromechanical coupling factor, K_p, of 46% for BCTZ50 and 33% for BCTZ32 are obtained at room temperature, however, it strongly decreases upon increasing temperature toward T_c for both compositions. This behavior is expected in ferroelectric materials. In the following, we attempt to correlate the high piezoelectric effect to the high flexible polarization, based on ferroelectric hysteresis loops and pyroelectric current measurements.

D. Ferroelectric and pyroelectric characterizations

Figure 6(a) displays the temperature dependence of ferroelectric hysteresis loops for BCTZ50. In agreement with the literature, these P-E hysteresis loops are slim with low coercive fields of 1.61 kV cm^{-1} for BCTZ50 and 600 V cm^{-1} for BCTZ32 at RT. Figure 6(b) shows that the coercive field, E_c, for BCTZ50 rapidly decreases with an increase in temperature toward the ferroelectric transition compared to BCTZ32. These results give us a first indication that BCTZ are soft lead-free piezoceramics which exhibit a behavior in between relaxors and ferroelectrics. Pyroelectric experiments (Fig. 7) readily support this conclusion. In fact, the pyroelectric current is stable deep in the ferroelectric phase, leading to a continuous increase of the polarization [Fig. 7(a)]; no saturation could thus be reached, however, the maximum polarization stayed below 20 μC cm^{-2} for both compositions [Fig. 7(b)]. Reproducible steps could be detected in the polarization within the ferroelectric state. We ascribe such behavior to a sudden change within the ferroelectric domains. These may also be tentatively explained by the thermal activation among several equivalent ferroelectric states because of the proximity from the tricritical point. However, in the absence of detailed structural investigations, this question is left open at the present stage. At this point, we can thus summarize our results by saying that the polarization of BCTZ32 and BCTZ50 is very

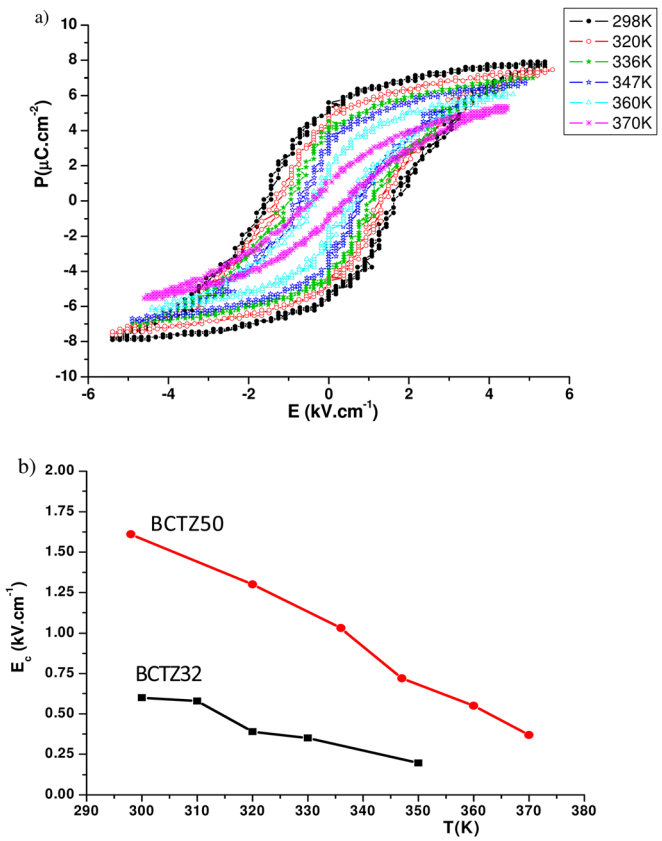

FIG. 6. (Color online) (a) Ferroelectric hysteresis loops for BCTZ50 recorded at different temperatures. (b) Thermal variation of the coercive field, E_c, for BCTZ50 and BCTZ32. The slim hysteresis loops of (a) result from the low coercive field of (b). The saturation polarization is reported in Fig. 7(b).

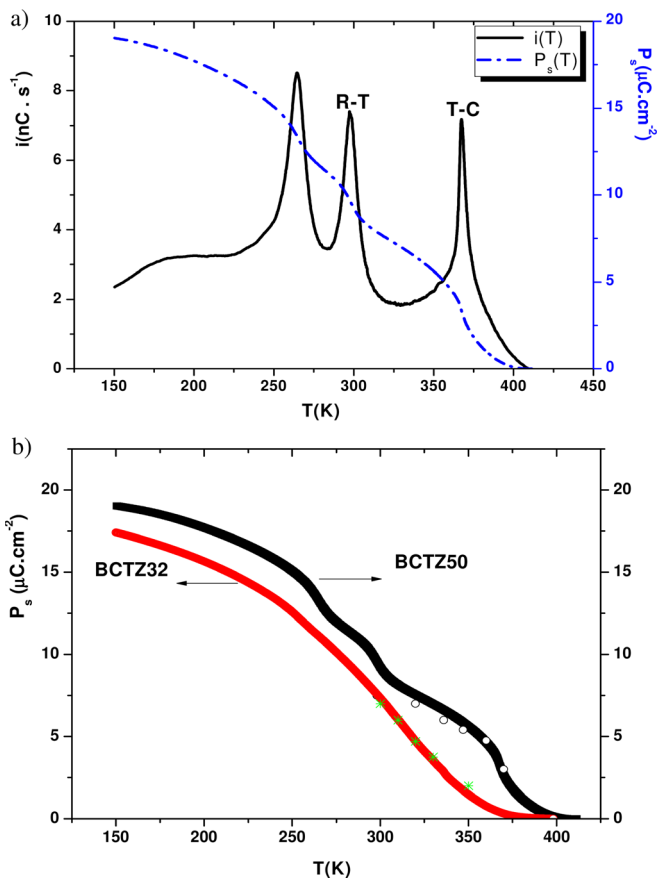

FIG. 7. (Color online) (a) Temperature dependence of the pyroelectric current, i, and the spontaneous polarization, P_s, for BCTZ50. (b) Spontaneous polarization vs temperature for BCTZ50 and BCTZ32. The open circles and the green stars correspond to the polarization saturation obtained from P-E hysteresis loops for these two compositions.

easily disturbed by temperature changes and its related coercitivity is extremely small. Even if the polarization reached is not high, its tuning by thermal and electric stresses is very easy. Our results thus strongly support high polarization flexibility as the main source of the strong piezoelectric coefficients in BCTZ ceramics. This critical situation (in the bidimensional T-x phase diagram) is similar to what was already observed in the best piezoelectric materials, PMN-PT.[23] In fact, it was shown that the electric field necessary for polarization rotation, and the energy barrier involved significantly decreased upon approaching a line of critical end points in the electric field-temperature-composition phase diagram, thus explaining the giant electromechanical response of these ferroelectric relaxors. Furthermore, this experimental work is in agreement with the theoretical model of the ultra-soft energy landscape for the polarization developed by Rossetti *et al.*[24] According to their work, the vanishing of the polarization anisotropy near the MPB line will result in a spherical degeneration of the energy surface leading to a polar glasslike state with no or very weak preferential polarization orientation. Consequently, the ferroelectric domains may show high mobility and unusual sensitivity to external stresses.

From the thermodynamic point of view, it should be noted that the previously proposed model was later supported by the work of Ren *et al*. in which extreme dielectric and piezoelectric properties for BCTZ ceramics were correlated with no or a very low energy barrier for polarization rotation between ⟨001⟩ tetragonal and ⟨111⟩ rhombohedral states at MPB line.[11] This behavior is mainly attributed to a flat free energy surface, especially for compositions close to the tricritical one.

IV. CONCLUSION

Using TiO_2 excess processed BCTZ ceramics, high piezoelectric responses were observed. Room temperature transverse piezoelectric coefficients, d_{31}, as high as 200 pC/N and 120 pC/N were measured for BCTZ50 and BCTZ32, respectively, which compare well with hard and soft PZT. To understand such an unusual piezoelectric effect, P-E hysteresis loops and pyroelectric current measurements were carried out. We found a behavior which is in between ferroelectrics and relaxors with highly flexible polarization versus thermal and electric stresses. The low coercive field offered an indication about the soft character of these materials.

Our results agreed with the model of vanishing polarization anisotropy near the MPB line which induces the near spherical degeneration of the energy surface. A small electric field, in this case, could drive the polarization rotation and gives rise to outstanding electromechanical properties.

More importantly, it should be kept in mind that the quest for promising lead-free candidates with high piezoelectric performance should converge to phase diagrams with the MPB line starting from a tricritical point where more than two structural phases can coexist. These complex situations will usually be required for the degeneration of the free energy surface and, therefore, for the high piezoelectric effect through a polarization rotation mechanism.

High-resolution synchrotron XRD measurements and others complementary analysis are being carried out to better understand structure property-relationships in BCTZ materials.

[1]L. Bellaiche and D. Vanderbilt, Phys. Rev. Lett. **83**, 1347 (1999).
[2]D. Damjanovic, J. Am. Ceram. Soc. **88**, 2663 (2005).
[3]M. Davis, D. Damjanovic, and N. Setter, J. Appl. Phys. **100**, 084103 (2006).
[4]W. Cao and E. Cross, Phys. Rev. B **47**, 4825 (1993).
[5]B. Noheda, D. E. Cox, G. Shirane, J. A. Gonzalo, L. E. Cross, and S.-E. Park, Appl. Phys. Lett. **74**, 2059 (1999).
[6]B. Noheda, J. A. Gonzalo, L. E. Cross, R. Guo, S.-E. Park, D. E. Cox, and G. Shirane, Phys. Rev. B **61**, 8687 (2000).
[7]J. Rödel, W. Jo, K. Seifert, E.-M. Anton, and T. Granzow, J. Am. Ceram. Soc. **92**, 1153 (2009).
[8]K. Higashide, K. I. Kakimoto, and H. Ohsato, J. Eur. Ceram. Soc. **27**, 4107 (2007).
[9]E. Hollenstein, D. Damjanovic, and N. Setter, J. Eur. Ceram. Soc. **27**, 4093 (2007).
[10]Y. Saito, H. Takao, T. Tani, T. Nonoyama, K. Takatori, T. Homma, T. Nagaya, and M. Nakamura, Nature (London) **432**, 84 (2004).
[11]W. Liu and X. Ren, Phys. Rev. Lett. **103**, 257602 (2009).
[12]W. Li, Z. Xu, R. Chu, P. Fu, and G. Zang, J. Am. Ceram. Soc. **93**, 2942 (2010).
[13]H. Bao, C. Zhou, D. Xue, J. Gao, and X. Ren, J. Phys. D: Appl. Phys. **43**, 465401 (2010).
[14]J. Ravez, C. Broustera, and A. Simon, J. Mater. Chem. **9**, 1609 (1999).
[15]IEEE Standard on Piezoelectricity, ANSI/IEEE Std. 176-1987.
[16]R. D. Shannon and C. T. Prewitt, Acta Crystallogr., Sect. B: Struct. Cryst. Chem. B25, 925 (1969).
[17]R. D. Shannon, Acta Crystallogr., Sect. A: Cryst. Phys., Diffr., Theor. Gen. Crystallogr. A32, 751 (1976).
[18]T. L. Rhyne, IEEE Trans. Sonics Ultrason. **SU25**, 2 (1978).
[19]C. A. Randall, N. Kim, J.-P. Kucera, W. Cao, and T. R. Shrout, J. Am. Ceram. Soc. **81**, 677 (1998).
[20]J. F. Tressler, S. Alkoy, and R. E. Newnham, J. Electroceram. **4**, 257 (1998).
[21]R. G. Sabat, B. K. Mukherjee, W. Ren, and G. Yang, J. Appl. Phys. **101**, 064111 (2007).
[22]H. Fu and R. E. Cohen, Nature (London) **403**, 281 (2000).
[23]Z. Kutnjak, J. Petzelt, and R. Blinc, Nature (London) **441**, 956 (2006).
[24]G. A. Rossetti, Jr., A. G. Khachaturyan, G. Akcay, and Y. Ni, J. Appl. Phys **103**, 114113 (2008).